Available online at www.sciencedirect.com
ScienceDirect
Physics Letters A 372 (2008) 1070–1076
PHYSICS LETTERS A
www.elsevier.com/locate/pla

Analysis and circuit realization of intermittency with multiple laminar states

Qingfei Chen [a], Yiguang Hong [b,*], Guanrong Chen [c], Shijian Cang [d], Qiuhai Zhong [e]

[a] *Department of Electrical Engineering, Arizona State University, Tempe, AZ 85287, USA*
[b] *Institute of Systems Science, Chinese Academy of Sciences, Beijing 10080, China*
[c] *Department of Electronic Engineering, City University of Hong Kong, Hong Kong SAR, China*
[d] *Department of Automation, Nankai University, Tianjin 300070, China*
[e] *Department of Automatic Control, Beijing Institute of Technology, Beijing 10083, China*

Received 20 March 2007; received in revised form 30 August 2007; accepted 10 September 2007

Available online 14 September 2007

Communicated by A.R. Bishop

Abstract

In this Letter, an electrical circuit is built for realizing the multi-state intermittency generated by a simple force-driven chaotic system. The intermittency phenomenon and its underlaying mechanism are analyzed, and the experimental results are discussed. It is shown that, with two classes of invariant subspaces, the number of the laminar states and the distance between the adjacent laminar states of the created multi-state on-off intermittency can be arbitrarily changed by manipulating the control parameters.

PACS: 05.45.-a; 05.45.Gg

Keywords: Multi-state intermittency; Chaotic systems; Circuit realization; Transverse stability

1. Introduction

Intermittency is an important and interesting chaos-related phenomenon, which has attracted increasing attention from scientists and engineers in various fields (e.g., [1–4]). In addition to the well-known three simple types of intermittencies [5], on-off intermittency is one of the popular intermittencies found in a variety of coupled or force-driven nonlinear systems. Its dynamical behaviors and underlying mechanism have been widely noticed and systematically explored. This intermittency, with two distinguished phases: the burst phase ("on" state) and the laminar phase ("off" state, is naturally related to the transverse instability of chaotic attractors confined to some invariant manifolds of lower dimensions in the phase space [6]. In addition, other intermittent phenomena such as the crisis-induced intermittency [7] and in-out intermittency [3,8] are being found or constructed recently, one after another. Since chaos-related intermittency is "useful" in many research areas, the control or generation of various intermittencies may be worked out by exploring the intrinsic nonlinear structures of the underlying natural or man-made systems as done in conventional chaos control [9–12].

One particular type of intermittency is the multi-state (on-off) intermittent phenomena, which have been found in many physical systems, for example, the two-state on-off intermittency studied in [13] and the multi-state intermittency with infinite states discussed in [14], where infinitely many lower-dimensional symmetric invariant subspaces exist in the considered intermittent system. In such studies, the Duffing oscillator was usually employed to drive the system to create multi-state intermittency. This type of intermittency phenomena were also observed in the collective behaviors of mass-migrating animal groups [1]. Moreover, as found in this Letter, it naturally leads to multi-scroll chaotic attractors, which have been widely discussed in recent years (see [11,12] and many references therein).

In the pursuit of further understanding intermittencies, a notable new trend is to take advantage of the continual growth

* Corresponding author.
E-mail address: yghong@iss.ac.cn (Y. Hong).

0375-9601/$ – see front matter
doi:10.1016/j.physleta.2007.09.018

of knowledge on nonlinearity and complexity thereby building some man-made systems that can display various intermittencies. In this endeavor, building circuits is a typical physics and engineering approach; examples include type-I or type-II intermittencies demonstrated in some nonlinear circuits [15,16]. Although many works with circuit implementation have been done for intermittencies and multi-scroll chaos [11,12], there are no circuit realizations reported for generating multi-state intermittency (along with multi-scroll attractor) to the best of our knowledge.

In this Letter, a nonlinear system is introduced and analyzed for generating multi-state on-off intermittency at first. Then stability and control problems of these intermittency phenomena are then discussed. Moreover, circuit realization and corresponding experiments are carried out to confirm the observed multi-state intermittent phenomena and related multi-scroll orbits.

2. Multi-state intermittency and invariant manifolds

Consider a second-order system,

$$\frac{d^2}{dt^2}y = -\gamma\frac{d}{dt}y - 4F(ey)(x-\alpha), \tag{1}$$

where γ is the friction coefficient, α and e are control parameters, and F is a continuous window-modulating function given by

$$F(\theta) = \begin{cases} 1 & \text{if } \theta > 2n_1\pi + \pi/2, \\ -1 & \text{if } \theta < -2n_2\pi - \pi/2, \\ \sin(\theta) & \text{otherwise}, \end{cases} \tag{2}$$

in which integers n_1 and n_2 are window-size parameters satisfying $n_1 + n_2 \geqslant 0$.

Let system (1) be driven by the following Duffing oscillator:

$$\frac{d^2}{dt^2}x = -\gamma\frac{d}{dt}x + 4x\left(1-x^2\right) + \rho\sin(\omega t), \tag{3}$$

where ω is the frequency of the oscillation.

By setting

$$v_x = \frac{dx}{dt}, \qquad v_y = \frac{dy}{dt}, \qquad z = \omega t,$$

one can rewrite the force-driven system (1) with (3) as the following system:

$$\begin{cases} \frac{dx}{dt} = v_x, \\ \frac{dv_x}{dt} = -\gamma v_x + 4x(1-x^2) + \rho\sin z, \\ \frac{dz}{dt} = \omega, \\ \frac{dy}{dt} = v_y, \\ \frac{dv_y}{dt} = -\gamma v_y - 4F(ey)(x-\alpha). \end{cases} \tag{4}$$

To study the underlying dynamical mechanism, the invariant manifolds of system (4) is first analyzed. In so doing, by letting $dy/dt = 0$ and $dv_y/dt = 0$ one can obtain two classes of invariant subspaces of system (4), as follows:

$$\text{Class 1:} \quad H_k^1 = \left\{(x, v_x, y, v_y, z) \mid v_y = 0,\ y = \frac{2k\pi}{e}\right\}, \tag{5}$$

where $k = -n_2, -n_2+1, \ldots, 0, \ldots, n_1-1, n_1$ (that is, there are $n_1 + n_2 + 1$ Class 1 subspaces);

$$\text{Class 2:} \quad H_k^2 = \left\{(x, v_x, y, v_y, z) \mid v_y = 0,\ y = \frac{2k\pi + \pi}{e}\right\}, \tag{6}$$

where $k = -n_2, -n_2+1, \ldots, 0, \ldots, n_1-1$ (that is, there are $n_1 + n_2$ Class 2 invariant subspaces).

In each of the above two invariant subspaces, there is a chaotic attractor resulting from the Duffing equations, implying that the intermittency is "on-off" type according to its definition.

First, consider the simple case of the on-off intermittency with infinitely many laminar states. Set $n_1 = n_2 = \infty$; that is, $F(ey) = \sin(ey)$. Then, one has

$$\begin{cases} H_k^1 = \{(x, v_x, y, v_y, z) \mid v_y = 0,\ y = \frac{2k\pi}{e}\}, \\ H_k^2 = \{(x, v_x, y, v_y, z) \mid v_y = 0,\ y = \frac{(2k+1)\pi}{e}\} \end{cases} \tag{7}$$

for all integers $k = 0, \pm1, \pm2, \ldots$.

In analyzing the Transverse Lyapunov Exponents (TLE) on these invariant manifolds H_k^1 and H_k^2, one has

$$\begin{cases} \dot{\delta}y^1 = \delta v_{y^1}, \\ \dot{\delta}v_{y^1} = -4e(x-\alpha)\delta y^1 - \gamma\delta v_{y^1}, \end{cases} \tag{8}$$

for H_k^1, and

$$\begin{cases} \dot{\delta}y^2 = \delta v_{y^2}, \\ \dot{\delta}v_{y^2} = 4e(x-\alpha)\delta y^2 - \gamma\delta v_{y^2}, \end{cases} \tag{9}$$

for H_k^2, respectively. The maximum Lyapunov exponents $h_\perp^1$ and $h_\perp^2$ (i.e., the TLE), corresponding to the respective invariant manifolds H_k^1 and H_k^2, can be numerically calculated by the formula $h_\perp^{1,2} = \lim_{t\to\infty}\ln(\delta^{1,2}(t)/\delta^{1,2}(0))/t$, where $\delta^{1,2}(t) = \sqrt{\delta y^{1,2}(t)^2 + \delta v_{y^{1,2}}(t)^2}$ [7,13]. In our calculation, we set the parameters as

$$\gamma = 0.05, \qquad \omega = 3.5, \qquad \rho = 2.3, \qquad e = 1. \tag{10}$$

Figs. 1(a) and (b) show the changes of $h_\perp^i$ $(i = 1, 2)$. It can be seen that, as α increases in the interval $[-2.6, -2]$, $h_\perp^1$ changes from negative to positive at the critical point $\alpha_c^1 \approx -2.07$ and $h_\perp^2$ remains positive in this interval.

Since the Duffing oscillator (3) is invariant under the transformation $(x, v_x, z) \to (-x, -v_x, z+\pi)$, one may take $x = -x'$, $v_x = -v_{x'}$, $z = z' + \pi$ so that system (4) with $F(y) = \sin(y)$ can be rewritten as

$$\begin{cases} \frac{d}{dt}x' = v_{x'}, \\ \frac{d}{dt}v_{x'} = -\gamma v_{x'} + 4x'(1-x'^2) + \rho\sin z', \\ \frac{d}{dt}z' = \omega, \\ \frac{d}{dt}y = v_y, \\ \frac{d}{dt}v_y = -\gamma v_y - 4\sin(ey)(-x'-\alpha). \end{cases} \tag{11}$$

Similarly, one obtains

$$\begin{cases} \dot{\delta}y^1 = \delta v_{y^1}, \\ \dot{\delta}v_{y^1} = 4e(x'+\alpha)\delta y^1 - \gamma\delta v_{y^1}, \end{cases} \tag{12}$$

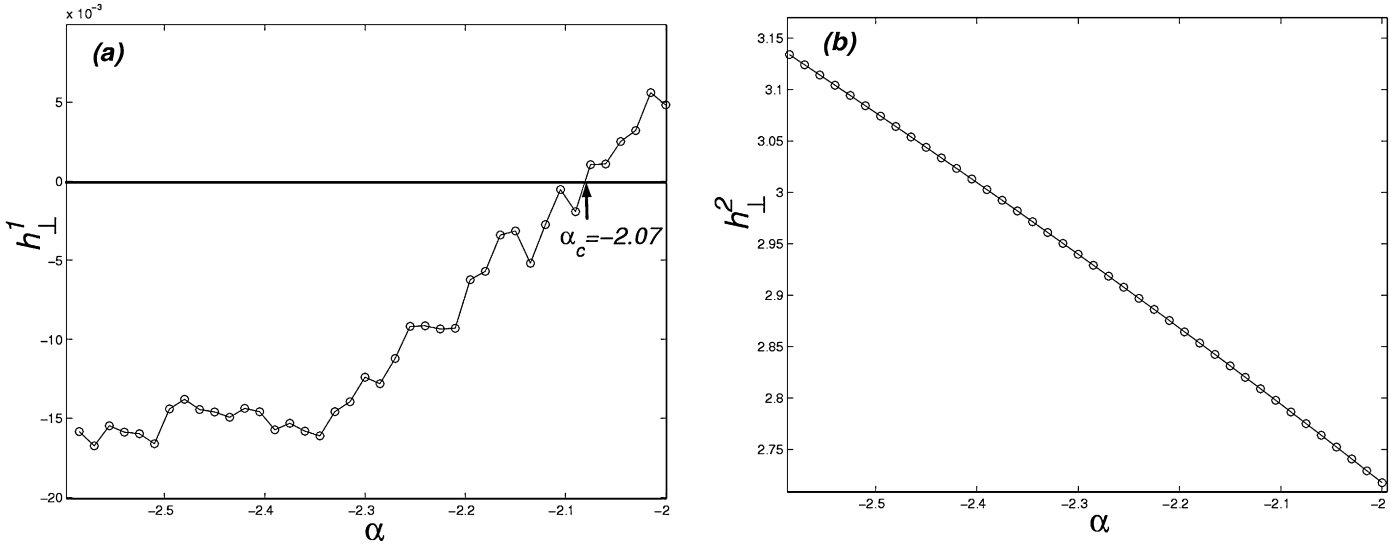

Fig. 1. Transverse Lyapunov exponents of H_i^1 and H_i^2 versus α.

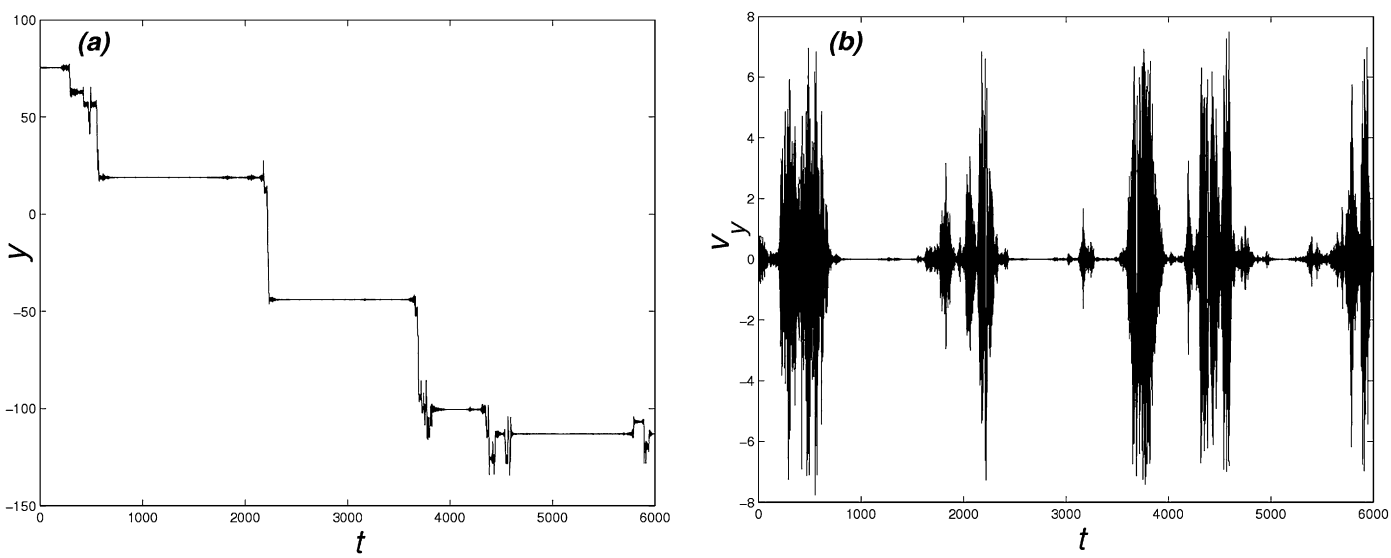

Fig. 2. Time series of $y(t)$ and $v_y(t)$ when $\alpha = -2$.

for H_k^1, and

$$\begin{cases} \dot{\delta} y^2 = \delta v_{y^2}, \\ \dot{\delta} v_{y^2} = -4e(x' + \alpha)\delta y^2 - \gamma \delta v_{y^2}, \end{cases} \tag{13}$$

for H_k^2, respectively. Note that (12) (or (13)) becomes (9) (or (8)) if one substitutes α by $-\alpha$. Therefore, the TLE of H_k^1 with α is equal to that of H_k^2 with $-\alpha$, which implies that the critical point of H_k^2 for $h_\perp^2$ is $\alpha_c^2 = -\alpha_c^1 \approx 2.07$.

Define another TLE $\hat{h}_\perp^1 = \max_{(x(0),v_x(0),z(0))\in A} h_\perp^1(x(0), v_x(0), z(0))$, where A denotes the chaotic attractor with respect to the indicated initial conditions [7]. If $\hat{h}_\perp^1 > 0$ over a zero measure set of points in A and $h_\perp^1 < 0$ for some $x(0)$, $v_x(0)$, $z(0)$ in H_k^1, whereas H_k^2 are all unstable near $\alpha = \alpha_c^1$. If α is slightly larger than α_c^1, then $h_\perp^1$ becomes positive and on-off intermittency emerges [7].

For system (4), $y(t)$ has infinitely many laminar states of on-off intermittency as $y(t)$ jumps unpredictably among all the invariant manifolds, though $v_y(t)$ has only one single laminar state of on-off intermittency, as shown in Figs. 2(a) and (b), where $\alpha = -2 > \alpha_c^1$. Fig. 2(a) demonstrates that $y(t)$ has a step-like behavior, a typical random-walk motion among different laminar states, corresponding to the invariant manifolds H_k^1 with different values of k.

3. Stability and control of finite-state intermittency

In the last section, $F(y) = \sin(y)$ was chosen to generate infinitely many laminar states of on-off intermittency. Here, the function $F(y)$ in (2) is used, with suitably selected "window-size" integers n_1 and n_2, which can generate any number of laminar states in a desired range by removing or shielding off unfavorable invariant manifolds.

Return to system (4). As discussed above, the second class of invariant subspaces (i.e., H_k^2 for some integer k) are unstable when α is close to α_c^1. Therefore, if α is slightly smaller than α_c^1, then intermingled basins of attraction in the subspaces H_k^1 ($k = -n_2, -n_2+1, \ldots, 0, \ldots, n_1-1$) appear (therefore, there is no intermittency); if α is slightly larger than α_c^1, then (n_1+n_2+1) laminar states of the intermittency of $y(t)$ can be visualized, precisely with the following levels of laminar states:

$$y(t) = \frac{2k\pi}{e}, \quad k = -n_2, -n_2+1, \ldots, 0, \ldots, n_1-1, n_1. \tag{14}$$

Clearly, the number of laminar states can be easily controlled by manipulating n_1 and n_2. Take $\alpha = -1.905 > \alpha_c$, Fig. 3 shows a three-state on-off intermittency with $n_1 = n_2 = 1$. Moreover, Figs. 4(a) and (b) show the cases of 5-state (with $n_1 = 2$, $n_2 = 2$) and 9-state (with $n_1 = 4, n_2 = 4$) intermittencies, respectively. From these figures, one can see that differing from the single-state on-off intermittency, $y(t)$ jumps out occasionally from the steady "off" states (laminar states) to the irregular "on" states and then quickly goes back to one of the "off" states ($y = \frac{2k\pi}{e}$, $k = -n_2, -n_2+1, \ldots, 0, \ldots, n_1-1, n_1$).

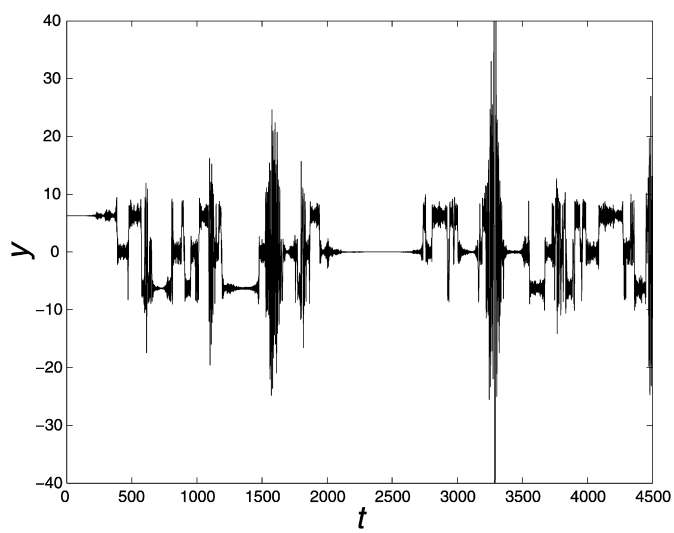

Fig. 3. Three-state on-off intermittency: $n_1 = n_2 = 1$.

Furthermore, it would be interesting to analyze why the intermittency trajectory can be kept around a given region determined by n_1 and n_2. Here, by the virtue of the simple structure of system (4), the stability of this (n_1+n_2+1)-state on-off intermittency is discussed, under the following condition:

$$\alpha < 0, \qquad \gamma > 0. \tag{15}$$

Define three intervals:

$$\Delta = \left[\frac{-2n_2\pi - \frac{\pi}{2}}{e}, \frac{2n_1\pi + \frac{\pi}{2}}{e}\right],$$
$$\Delta_+ = \left(\frac{2n_1\pi + \frac{\pi}{2}}{e}, +\infty\right),$$
$$\Delta_- = \left(-\infty, \frac{-2n_2\pi - \frac{\pi}{2}}{e}\right).$$

If $y \in \Delta$, then $F(ey) = \sin(ey)$ and there are laminar states at $y = \frac{2k\pi}{e}$ ($k = -n_2, -n_2+1, \ldots, 0, \ldots, n_1-1, n_1$) due to the occurrence of a blowout bifurcation, following a similar analysis given in the last subsection. In fact, $y(t)$ can return to interval Δ after $y(t)$ walks out of Δ irregularly.

First, consider the case of $y(t_0) \in \Delta_+$, where $F(ey) = 1$ and system (4) becomes

$$\begin{cases} \frac{d}{dt}x = v_x, \\ \frac{d}{dt}v_x = -\gamma v_x + 4x(1-x^2) + \rho \sin z, \\ \frac{d}{dt}z = \omega, \\ \frac{d}{dt}y = v_y, \\ \frac{d}{dt}v_y = -\gamma v_y - 4(x-\alpha). \end{cases} \tag{16}$$

The last two equations of system (16) can be rewritten as

$$\begin{pmatrix} \dot{y} \\ \dot{v}_y \end{pmatrix} = \begin{pmatrix} 0 & 1 \\ 0 & -\gamma \end{pmatrix} \begin{pmatrix} y \\ v_y \end{pmatrix} + \begin{pmatrix} 0 \\ 1 \end{pmatrix} u(t), \quad u(t) = -4\big(x(t) - \alpha\big). \tag{17}$$

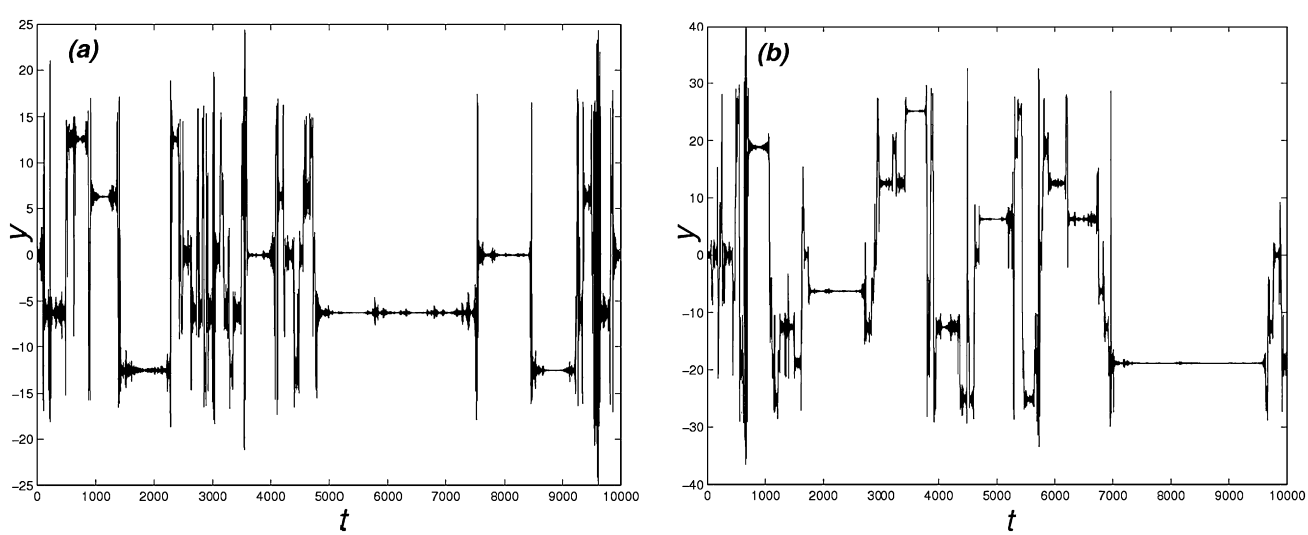

Fig. 4. Five-state and nine-state on-off intermittencies: (a) $n_1 = n_2 = 2$; (b) $n_1 = n_2 = 4$.

Solving (17) gives

$$y = R_1 + R_2 \tag{18}$$

where

$$R_1 = y(t_0) + \frac{1}{\gamma}\left(1 - e^{-\gamma(t-t_0)}\right)v_y(t_0) - \int_{t_0}^{t} \frac{1}{\gamma} e^{-\gamma(t-\tau)} u(\tau)\, d\tau,$$

and

$$R_2 = \frac{1}{\gamma}\int_{t_0}^{t} u(\tau)\, d\tau.$$

Clearly, R_1 is bounded since $|u(\tau)|$ is bounded (noticing that the Duffing attractor is bounded), say $|u(\tau)| \leqslant M$, for some constant $M > 0$. Obviously,

$$\begin{aligned} |R_1| &\leqslant \left|y(t_0)\right| + \left|\frac{1}{\gamma}\left(1 - e^{-\gamma(t-t_0)}\right)v_y(t_0)\right| + \frac{M}{\gamma}\int_{t_0}^{t} e^{-\gamma(t-\tau)}\, d\tau \\ &\leqslant \left|y(t_0)\right| + \frac{1}{\gamma}\left|v_y(t_0)\right| + \frac{M}{\gamma^2}. \end{aligned}$$

Furthermore, considering the Duffing oscillator (3) with $x(t)$ being bounded and symmetric to $\{(x, v_x) \mid x = 0, v_x = 0\}$, one has, by (15),

$$R_2 = \frac{1}{\gamma}\left(\int_{t_0}^{t} -4x(t)\, dt + 4\alpha(t - t_0)\right) \sim \frac{4\alpha}{\gamma} t \to -\infty,$$

as $t \to \infty$. Therefore, for system (16), $y(t) \to -\infty$ as $t \to \infty$ under condition (15). This implies that $y(t)$ cannot stay in Δ_+ forever but must go back to Δ in some intervals of time.

Similarly, still under condition (15), when $y(t_0)$ is in Δ_-, $F(ey) = -1$ ($F(ey) = 1$ when $y(t_0)$ belongs to Δ_+). With the condition that $\alpha < 0$, $R_2 = 1/(\gamma)\int_{t_0}^{t} u(\tau)\, d\tau = 1/(\gamma)(\int_{t_0}^{t} 4x(t)\, dt - 4\alpha(t - t_0)) \sim -4\alpha/(\gamma)t \to \infty$ as $t \to \infty$. Because R_1 which is irrelevant to y is bounded as discussed before, $y(t) = R_1 + R_2 \to \infty$ as $t \to \infty$. Since $\Delta_- < \Delta < \Delta_+$, one can conclude that in some interval of time, $y(t)$ will go back to Δ. In other words, $y(t)$ will go back to Δ again in a finite time. Thus, the intermittency is verified to stay in Δ most of time.

In addition, the distance between the adjacent laminar states of the created multi-state on-off intermittency attractors can also be easily adjusted. In fact, from (5) and (6), the distance can be written as:

$$d = \left|\sqrt{\left((v_y)^2 + y^2\right)\big|_{k=n}} - \sqrt{\left((v_y)^2 + y^2\right)\big|_{k=n+1}}\right| = 2\pi/e$$

which is based on parameter e in control function $F(ey)$.

It is now understood that the multi-state intermittency is typically involved with multiple (unstable) "attractors" in multiple invariant manifolds of a dynamical system when the transverse Lyapunov exponents (TLE) of these manifolds become slightly positive. These "attractors" interconnected each other forming multiple scrolls. The generation mechanism of multi-scroll attractors has been studied in many works (e.g. [11,12]) and here multi-state intermittency provides another approach to create multi-scroll attractors (see the figures of circuit experiments in the next section. For space limitations, we do not mention much about multi-scroll attractors here).

4. Circuit implementation of the intermittency model

In this section, a circuit for system (4) is built to demonstrate the step-like multi-state intermittency observed and analyzed above.

A circuit implementation of system (4), which consists of (1) and (3), is shown in Fig. 5. The upper part of the electronic diagram (above dot-and-dash line) is corresponding to the driving system (i.e., Duffing oscillator (3)), while the lower part (below dot-and-dash line), to the driven system (1). The circuit is made of four channels to conduct the integration of the four state variables, x, v_x, y, and v_y, respectively. The operational amplifiers LF347 and the associated circuitry perform the basic operations of addition, subtraction, and integration. The nonlinear terms of system (4) are implemented with the analog multipliers AD633 and the highly accurate universal trigonometric function converter AD639.

In the following experiments, $\gamma = 0.05$, $\omega = 3.5$, $\rho = 2.3$, and $e = 1$, as in (10). And γ in the second equation of system (4) is realized by resistors R9 and R11, while γ in the fifth equation is realized by resistors R26 and R27. Moreover, ρ is the amplitude of the driving signal $2.3\sin(2\pi f)$, with $\omega = 2\pi f$.

Here, parameter ω needs to be explained in more details. When $\omega = 3.5$, one has $f = 0.577$ Hz. As is well known, it is hard to realize the signal with such a low frequency by an electronic circuit; therefore, accordingly a linear transform for ω is adopted, magnifying it by 100 times with a change of the sizes of the capacitors C1, C2, C3, and C4 that have been labeled in Fig. 5. In particular, a 57.7 Hz signal is used as the driving signal, which can be easily obtained by various function generators. With this frequency signal and the circuit elements labeled in Fig. 5, the physical attribute of system (4) does not change. Additionally, the parameter α of system (4) is governed by resistor R28 and R29, and their relationship is known as follows:

$$\mathrm{R28} = -\frac{20 + 4\alpha}{\alpha}\ (\mathrm{k}\Omega).$$

Since R28 is nonnegative, the value range of α is within $[-5, 0)$. In other words, the change of the parameter α in system (4) can be implemented by adjusting the linear resistor in Fig. 5.

In the practical tests, the linear resistor was taken to be $\mathrm{R28} = 6.5\ \mathrm{k}\Omega$, which means $\alpha = -1.905$. Then, the parameters n_1 and n_2 of the driving signal were adjusted, as discussed in the preceding sections. For example, with setting $n_1 = n_2 = 1$, $n_1 = n_2 = 3$, $n_1 = 5, n_2 = 4$, and $n_1 = n_2 = 6$, Fig. 6 clearly demonstrates the corresponding 3-, 7-, 10-, and 13-states on-off intermittencies, respectively, which were recorded by the Tektronix color digital oscilloscope TDS2024.

All results obtained above show step-like multi-state intermittent behaviors and confirm the analysis given in the preceding section. Note that the experimental results reported above

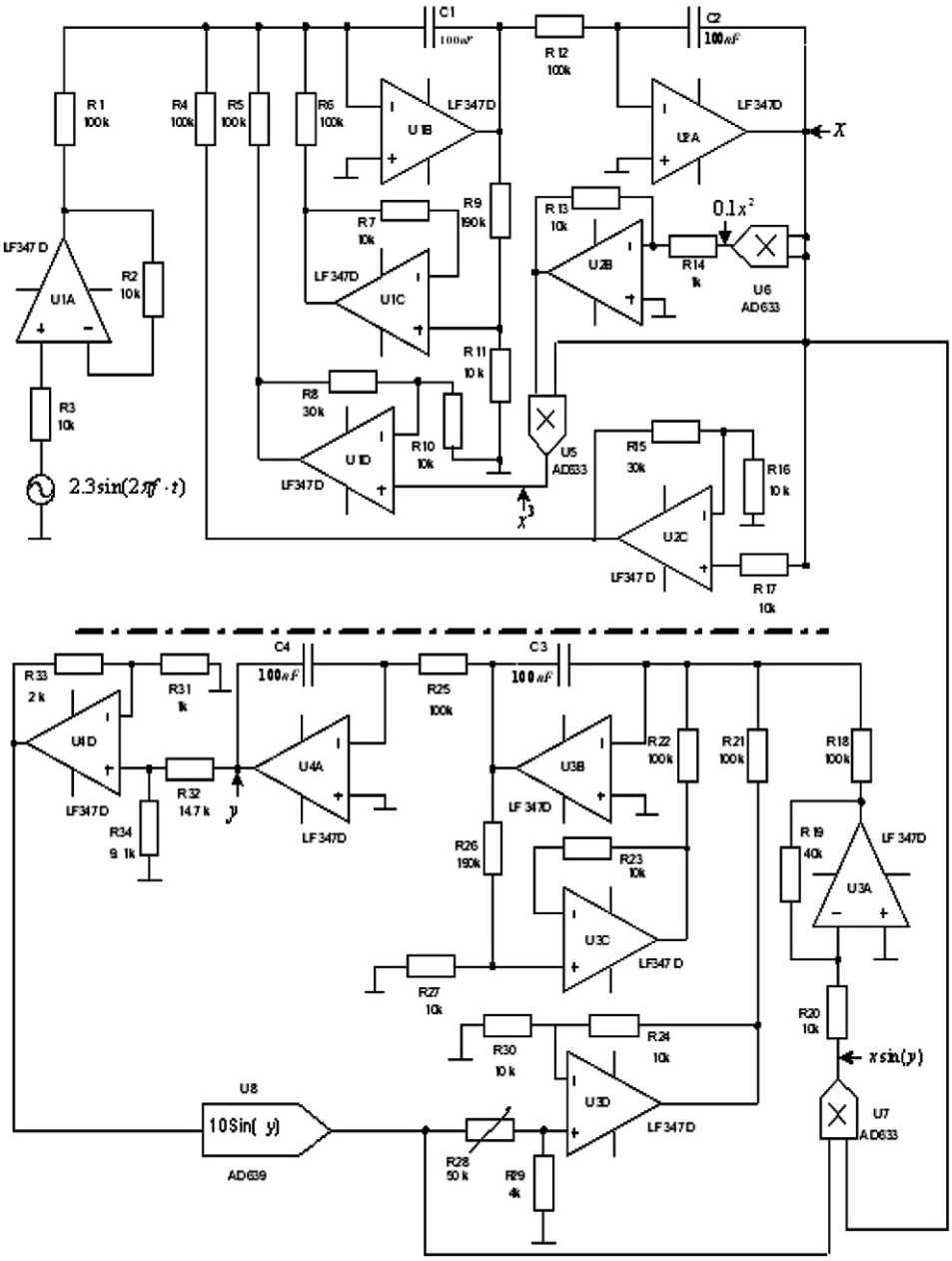

Fig. 5. Electronic circuit described by (1) and (3).

are not exactly the same as the numerical results though the parameters may be taken the same values, as commonly experienced in many case studies between numerical simulations and laboratory experiments. As a matter of fact, the on-off intermittency pattern is also sensitive to tiny changes of initial conditions (or during the evolution), and modeling errors and environmental noise are unavoidable in hardware experiments.

It can be observed that, in this intermittent phenomenon, there are chaotic attractors located in the multiple invariant subspaces. Each attractor is not transversely stable and, therefore, the orbits around these (unstable) attractors "entangle" each other to shape a stable intermittent attractor. In other words, these interconnected (unstable) attractors help construct a stable intermittency attractor with multiple scrolls in the phase space. As a result, the occurrence of a multi-state intermittency, attributed to the attractors in the multiple invariant manifolds over time, naturally implies the existence of multi-scroll (chaotic) attractors in the phase space (y, v_y), as verified by Fig. 7. In other words, the multi-state intermittency may provide another route to the creation of multi-scroll attractors, as discussed in [11,12].

5. Conclusions

In this Letter, the generation and some basic properties of multi-state on-off intermittency have been studied based on a simple nonlinear system. It is shown that the number of laminar states and the distances between the adjacent states of the generated multi-state intermittency can be easily determined by tuning control parameters. A circuit has been built and some lab-based experiments have been carried out to confirm

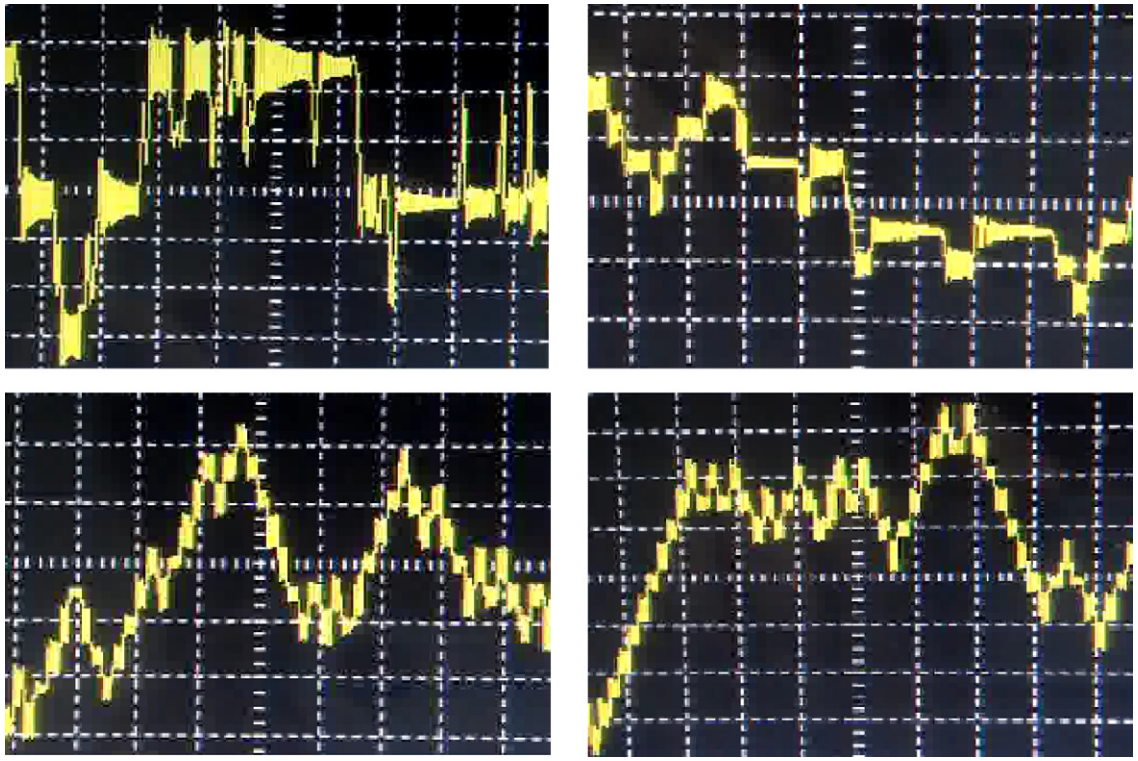

Fig. 6. Multi-state intermittency of the circuit: $y(t)$ vs. t.

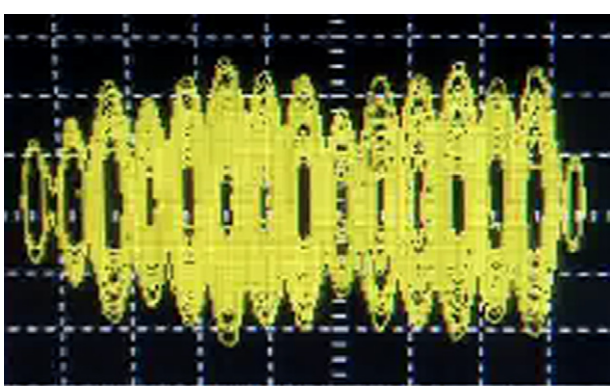

Fig. 7. Multi-state intermittency leads to a multi-scroll attractor.

various numerically-observed multi-state intermittent phenomena. Moreover, the multi-scroll attractor shown in the paper turns out to be a natural byproduct of a multi-state intermittency.

In fact, intermittency studies benefit much to the understanding of complex dynamics and critical nonlinear phenomena. New classes of intermittencies or new characteristics of the known intermittencies keep being discovered, which may lead to more practical applications. Additionally, simple circuit realization of specific intermittent phenomena plays an active role in the understanding of the intermittencies found in practical systems or in simulating the spikes observed in bio-systems such as biological neural networks, which may be beneficial to neural informatics or medicine-related high-tech developments. All these problems provide important yet nontrivial challenges, and some of them are currently under our investigations.

Acknowledgements

This work was supported by the NNSF of China under Grants 10472129, 60425307, 10475009, 50595411, and 60221301.

References

[1] J. Buhl, D. Stumpter, I. Couzin, J. Hale, E. Despland, E. Miller, S. Simpson, Science 312 (2006) 1402.
[2] J. Cabrera, J. Milton, Phys. Rev. Lett. 89 (2002) 1587.
[3] Q. Chen, Y. Hong, G. Chen, D. Hill, IEEE Trans. Circuits Systems-I 53 (2006) 2692.
[4] A. Pikovsky, J. Phys. A 16 (1984) 109.
[5] Y. Pomeau, P. Manneville, Commun. Math. Phys. 74 (1980) 189.
[6] N. Platt, E.A. Spiegel, C. Tresser, Phys. Rev. Lett. 70 (1993) 279.
[7] E. Ott, Chaos in Dynamical Systems, second ed., Cambridge Univ. Press, Cambridge, 2002.
[8] P. Ashwin, E. Covas, R. Tavakol, Phys. Rev. E 64 (2001) 204.
[9] G. Chen, X. Dong, From Chaos to Order, World Scientific, Singapore, 1998.
[10] Q. Chen, Y. Hong, G. Chen, Q. Zhong, Phys. Lett. A 348 (2006) 195.
[11] L. Chua, M. Komuro, T. Matsumoto, IEEE Trans. Circuits Systems 33 (1986) 1073.
[12] M. Yalcin, J. Suykens, J. Vandevalle, Cellular Neural Networks, Multi-Scoll Chaos and Synchronization, World Scientific, Singapore, 2005.
[13] Y.-C. Lai, C. Grebogi, Phys. Rev. E 52 (1995) R3313.
[14] M. Zhan, G. Hu, Phys. Rev. E 62 (2000) 375.
[15] M.S. Baptista, I.L. Calda, Physica D 132 (1999) 325.
[16] C. Kim, G. Yim, Y. Kim, J. Kim, H. Lee, Phys. Rev. E 56 (1997) 2593.